Journal of Molecular and Cellular Cardiology 89 (2015) 326–334

Contents lists available at ScienceDirect

Journal of Molecular and Cellular Cardiology

journal homepage: www.elsevier.com/locate/yjmcc

Calcium release near L-type calcium channels promotes beat-to-beat variability in ventricular myocytes from the chronic AV block dog

Gudrun Antoons [a,b,c,1], Daniel M. Johnson [a,1], Eef Dries [a], Demetrio J. Santiago [a], Semir Ozdemir [a,d], Ilse Lenaerts [a], Jet D.M. Beekman [b], Marien J.C. Houtman [b], Karin R. Sipido [a,*,2], Marc A. Vos [b,2]

[a] Experimental Cardiology, Department of Cardiovascular Sciences, KU Leuven (University of Leuven), Leuven, Belgium
[b] Department of Medical Physiology, Division of Heart and Lungs, University Medical Center Utrecht, University of Utrecht, Utrecht, The Netherlands
[c] Department of Physiology, Maastricht University, Maastricht, The Netherlands
[d] Department of Biophysics, Akdeniz University, Antalya, Turkey

ARTICLE INFO

Article history:
Received 18 March 2015
Received in revised form 8 September 2015
Accepted 6 October 2015
Available online 8 October 2015

Keywords:
Action potential
Repolarization variability
Remodeling
Proarrhythmia
Calcium handling

ABSTRACT

Beat-to-beat variability of ventricular repolarization (BVR) has been proposed as a strong predictor of Torsades de Pointes (TdP). BVR is also observed at the myocyte level, and a number of studies have shown the importance of calcium handling in influencing this parameter. The chronic AV block (CAVB) dog is a model of TdP arrhythmia in cardiac hypertrophy, and myocytes from these animals show extensive remodeling, including of Ca^{2+} handling. This remodeling process also leads to increased BVR. We aimed to determine the role that (local) Ca^{2+} handling plays in BVR.

In isolated LV myocytes an exponential relationship was observed between BVR magnitude and action potential duration (APD) at baseline. Inhibition of Ca^{2+} release from sarcoplasmic reticulum (SR) with thapsigargin resulted in a reduction of $[Ca^{2+}]_i$, and of both BVR and APD. Increasing I_{CaL} in the presence of thapsigargin restored APD but BVR remained low. In contrast, increasing I_{CaL} with preserved Ca^{2+} release increased both APD and BVR. Inhibition of Ca^{2+} release with caffeine, as with thapsigargin, reduced BVR despite maintained APD. Simultaneous inhibition of Na^+/Ca^{2+} exchange and I_{CaL} decreased APD and BVR to similar degrees, whilst increasing diastolic Ca^{2+}. Buffering of Ca^{2+} transients with BAPTA reduced BVR for a given APD to a greater extent than buffering with EGTA, suggesting subsarcolemmal Ca^{2+} transients modulated BVR to a larger extent than the cytosolic Ca^{2+} transient.

In conclusion, BVR in hypertrophied dog myocytes, at any APD, is strongly dependent on SR Ca^{2+} release, which may act through modulation of the L-type Ca^{2+} current in a subsarcolemmal microdomain.

© 2015 The Authors. Published by Elsevier Ltd. This is an open access article under the CC BY-NC-ND license (http://creativecommons.org/licenses/by-nc-nd/4.0/).

1. Introduction

The phenomenon of beat-to-beat variability of repolarization (BVR) can be observed at all levels of the cardiac hierarchy, from the action potential of single cardiac myocytes to the QT interval measured from ECG recordings. It has been previously shown that BVR is a better predictor of Torsades de Pointes (TdP) arrhythmia in a number of animal models and in selected patient populations when compared to repolarization prolongation alone [1–5].

Although it is likely that BVR is a result of complex interactions ranging from the ionic to the whole organ level, BVR of the single myocyte has been suggested to contribute to variability at the whole heart level. It is speculated that cellular BVR is driven by stochastic fluctuations in ion channel or transporter currents, and by the influence of local Ca^{2+} concentrations on ion channel activity. Despite the fact that these changes in current may be modest, they may have a significant impact on the duration of the ventricular AP plateau, where small changes in currents can have a large impact on voltage [5].

A number of recent studies have started to unravel the ionic mechanisms that influence the magnitude of BVR under various experimental conditions. For example, Johnson et al. [7] have previously illustrated that in un-remodeled canine ventricular myocytes sympathetic stimulation can rescue increased BVR induced by interventions that undermine the 'repolarization reserve', most likely due to β-adrenergic stimulation of the I_{Ks} current [8]. More recently the same group showed that under Ca^{2+} overloaded conditions induced by a combination of β-adrenergic stimulation and I_{Ks} block, BVR is driven by interspersed action potential

Abbreviations: AP, action potential; APD, action potential duration; BVR, beat-to-beat variability of repolarization; CAVB, chronic complete atrioventricular block; EAD, early after depolarization; LTCC, L-type Ca^{2+} channel; NCX, Na^+/Ca^{2+} exchanger; SR, sarcoplasmic reticulum; TdP, Torsades de Pointes.

* Corresponding author at: Department of Cardiovascular Sciences, Division of Experimental Cardiology, KU Leuven, Campus Gasthuisberg O/N1 704, Herestraat 49, Leuven B-3000, Belgium.
E-mail address: karin.sipido@med.kuleuven.be (K.R. Sipido).

[1] GA and DMJ contributed equally to this work.
[2] KS and MV share last authorship.

http://dx.doi.org/10.1016/j.yjmcc.2015.10.008
0022-2828/© 2015 The Authors. Published by Elsevier Ltd. This is an open access article under the CC BY-NC-ND license (http://creativecommons.org/licenses/by-nc-nd/4.0/).

prolongation caused by differences in Ca^{2+}-dependent inactivation of the L-type Ca^{2+} channel (LTCC) induced by spontaneous diastolic release events [9]. Buffering of intracellular Ca^{2+} either by EGTA or BAPTA-AM has also been shown to reduce BVR in un-remodeled myocytes, as has inhibition of the Na^+/Ca^{2+} exchanger (NCX) [6,7]. A separate study has also shown the importance of the late Na^+ current in determining BVR, especially when repolarization reserve is reduced and the net transmembrane current is small [10]. A number of computational studies have also investigated the relationship between stochastic ion channel gating and BVR [11,12]. These studies have shown stochastic gating of selected ion channels, notably (late) I_{Na} and I_{Ks}, could affect BVR. In addition Heijman et al. illustrated that although AP duration (APD) prolongation strongly increases BVR, it is not the sole determinant of exaggerated BVR where repolarization is compromised [13]. In this in silico study, action potential morphology and duration, as well as beat-to-beat fluctuations in intracellular Ca^{2+} were shown to be important determinants of BVR magnitude, in addition to stochastic channel gating.

The dog with chronic complete AV block (CAVB) is a well-characterized model for arrhythmias, related to structural and electrical remodeling including prolonged repolarization times and bi-ventricular hypertrophy [14]. These animals are more susceptible for TdP arrhythmia under various conditions. At the cellular level, I_{Ks} is reduced, whereas SR Ca^{2+} release, NCX and the Ca^{2+} window current are enhanced [15–17].

Furthermore the CAVB heart is predisposed to delayed afterdepolarization dependent ventricular arrhythmias when challenged with positive inotropes [18]. Interestingly the relationship between intracellular Ca^{2+} and frequency is inverted in CAVB when compared with normal sinus rhythm, with higher sarcoplasmic reticulum Ca^{2+} concentrations occurring at slower heart rates [15]. In this model, BVR has been shown to be increased when compared to animals in normal sinus rhythm [19,20]. Furthermore BVR can distinguish animals that are susceptible to arrhythmia [21] and antiarrhythmic interventions significantly reduce BVR [21–23].

A number of studies have investigated cellular BVR in the CAVB myocytes, however the exact mechanisms behind BVR under these conditions remain elusive. Bourgonje et al. illustrated the importance of blockade of NCX with concomitant LTCC inhibition in preventing excessive BVR induced by I_{Kr} blockade [24]. Similar results were also seen after CAMKII inhibition with W7 or KN-93 [25]. Furthermore, similar to data in un-remodeled myocytes, late Na^+ channel inhibition with ranolazine or a combination of Ca^{2+} channel inhibition together with late Na^+ inhibition using flunarizine was able to reduce BVR in the CAVB myocytes [22,23]. However in all of these studies the decrease in BVR was accompanied by a decrease in APD, making it difficult to dissect out the contribution of this component compared to other possible factors that underlie the changes observed in BVR.

Given the changes in Ca^{2+} handling in CAVB, and the fact that Ca^{2+} dependent currents have previously been implicated in the manifestation of BVR, the aim of the present study was to investigate how (local) Ca^{2+} release can influence cellular BVR in this model, with experiments aimed to dissect the role of SR Ca^{2+} release and of APD independently of one another. We have previously shown that modulation of LTCC by sarcoplasmic reticulum Ca^{2+} release in CAVB induces pronounced inactivation and recovery, and this within the dyadic subsarcolemmal space [17]. Therefore our working hypothesis is that variations in LTCC related to this local Ca^{2+}-dependent modulation are an important mechanism contributing to BVR during the action potential.

2. Methods

2.1. Animal model

After sedation with 0.5 mg/kg methadone, 0.5 mg/kg acepromazine and 0.5 mg atropine i.m. general anesthesia was induced by sodium pentobarbital (25 mg/kg i.v.) and maintained with inhaled isoflurane (1.5% in N_2O/O_2 (2:1)) in a total of 30 adult mongrel dogs (Marshall Bioresources, NY, USA). Once under complete anesthesia, radiofrequency ablation of the His bundle was used to create CAVB as previously described [26,27]. Proper care was taken before, during and after the experiments, including a thermal mattress to maintain body temperature, fluid administration to avoid volume depletion (0.9% NaCl) and administration of analgesia (buprenorphine, 0.015 mg/kg i.m.) and antibiotics (ampicillin, 1000 mg i.m. pre and post-operative). Animal studies conformed to the Guide for the Care and Use of Laboratory Animals. Experiments were approved by The Committee for Experiments on Animals of Utrecht University, the Netherlands. Animal handling was in accordance with the European Directive for the Protection of Vertebrate Animals used for Experimental and Other Scientific Purposes (2010/63/EU).

2.2. Cell isolation

Left ventricular myocytes were isolated as previously described [15]. Briefly, anesthesia was induced with pentobarbital (25 mg/kg), and the chest was opened via a left thoracotomy. After receiving 10 000 IU heparin (i.v.) hearts were excised and placed in O_2-gassed Ca^{2+} free standard buffer solution at approximately 4 °C. The circumflex coronary artery was cannulated and perfused. After ~20 min of collagenase perfusion and washout of enzyme, tissue was collected from the midmyocardial layer, after removal of the epicardial surface layer, and were then gently agitated, filtered and washed. LV myocytes were stored in standard buffer solution and were used within 48 h of isolation. Only rod shaped quiescent cells with clear striations were used for experiments.

2.3. Cellular electrophysiology

Experiments were performed at 37 °C. Cells were plated on a perfusion chamber placed on an inverted microscope (Nikon) equipped with a fluorescence system (Cairn Research Ltd). The setup allows for combined membrane currents and intracellular calcium $[Ca^{2+}]_i$ recording using either Indo-1 AM or K_5 Fluo-4. For the Indo-1 experiments the dye was excited at 365 nm. The fluorescence signal was expressed as the ratio of emitted fluorescence at 410 and 485 nm. Action potentials were recorded during steady-state stimulation with 2-ms current injections using the microelectrode technique for minimal disturbance of the intracellular environment. Microelectrodes had a resistance of 30–50 MΩ when filled with 3 M KCl. In some experiments, action potentials were measured in whole-cell current-clamp using the amphotericin-B perforated patch technique. This configuration allowed switching from current-clamp to AP clamp or voltage clamp mode. Patch pipettes filled with internal solution had a resistance of 1.5 to 3 MΩ. Transmembrane potentials and currents were sampled and digitized at 4 kHz (PClamp 8 or 9, Axon instruments Inc.) In a number of experiments, the whole-cell patch-clamp configuration was achieved and K_5Fluo-4 (0.05 mM) was included in the internal solution to simultaneous record Ca^{2+} transients as previously described [17]. In the Ca^{2+} buffering experiments, Ca^{2+} sensitive dye was omitted from the internal solution and either EGTA (10 mM) or BAPTA (10 mM) was included.

2.4. Drugs and experimental solutions

The external solution had the following composition (mM): NaCl 137, KCl 5.4, $MgCl_2$ 0.5, $CaCl_2$ 1.8, Na-HEPES 11.8 and glucose 10; pH 7.4 with NaOH. Using perforated patch, pipette solution contained (in mM): 130 KCl, 10 HEPES, 5 MgATP, 0.5 $MgCl_2$, 10 NaCl, 1 $CaCl_2$, and 0.00026 amphotericin B, pH adjusted to 7.20 using KOH. Internal solution for whole-cell patch clamp experiments contained (in mM): K-aspartate 120, NaCl 10, KCl 20, K-HEPES 10, and MgATP 5; pH 7.2. The Na^+–Ca^{2+} exchanger (NCX) was inhibited with 1 μM SEA0400

(Endotherm GmbH, Saarbrucken, Germany) SERCA was blocked using thapsigargin (Molecular Probes) which was prepared as a 1 mM stock solution in DMSO and diluted to a final concentration of 5 μM in Tyrode solution before use and BayK 8644 (Tocris Bioscience; 1 μM) was used as an agonist of the L-type Ca^{2+} current. Sustained caffeine application (10 mM, Sigma) was used to empty the sarcoplasmic reticulum of Ca^{2+}.

2.5. Data analysis and statistical comparisons

APD was quantified at 90% repolarization. BVR was quantified as short term variability of APD at 90% repolarization (APD_{90}): $\Sigma(|APD_{90}; i + 1 \text{ minus } APD_{90}; i|) / [nbeats \times \sqrt{2}]$ for 30 consecutive APs. [1] When applicable, data were reported as mean ± SEM of number experiments and significance was tested with either t-test or 1-way ANOVA. APD/BVR curves were generated by fitting the data to a monoexponential function and differences in the curve fits were tested by testing the residuals of the fit using the extra sum of squares F test. Differences were considered statistically significant if $P < 0.05$.

3. Results

3.1. Rate dependence of APD/BVR and Ca^{2+} transients in CAVB

Initially we investigated the relationship between APD, BVR and the underlying Ca^{2+} transient in myocytes isolated from the LV of CAVB animals under baseline conditions. Fig. 1A illustrates how BVR is altered as a function of stimulation frequency. Pacing the cells at 1 Hz led to an average APD of 334 ± 17 ms and BVR was 8 ± 0.8 ms (n = 24, N = 8) whilst, in the same cells at the slower stimulation frequencies of 0.25 Hz APD significantly increased to 445 ± 24 ms and BVR was also elevated to 15 ± 3.3 (n = 24, N = 8). As shown in Fig. 1B, the relationship between APD and BVR was not linear, and when data is plotted, from all cells at all stimulation frequency, could be fitted using a monoexponential ($R^2 = 0.62$) similar to findings in normal canine ventricular myocytes [13,28].

Consistent with our previous data Ca^{2+} transient amplitude was largest in CAVB at lower frequencies (Fig. 1A) [16]. At these low frequencies and long APD, variability was also clearly visible, but variability of the global Ca^{2+} transient was only visible in terms of duration, and not peak values. Under these conditions it is not possible to say if variability in Ca^{2+} is a cause of, or a result of, the variability in the APD. Furthermore it may be that the resolution of Ca^{2+} transient recordings was not high enough to detect any additional more subtle variability in Ca^{2+} transients. However, the examples illustrate that deviation and variability in APD are initiated early during the plateau, suggesting that modulation of plateau currents, possibly by Ca^{2+} release could be involved.

3.2. Modulating Ca^{2+} release can modulate BVR in CAVB myocytes

To tease out the mechanisms of how modulating Ca^{2+} release could alter BVR, specific pharmacological interventions were employed. Initially we used thapsigargin (5 μM) to block reuptake of Ca^{2+} into the SR, ultimately leading to an SR devoid of Ca^{2+}, thus effectively suppressing SR Ca^{2+} release during the AP. As shown in Fig. 2A after 5 min of

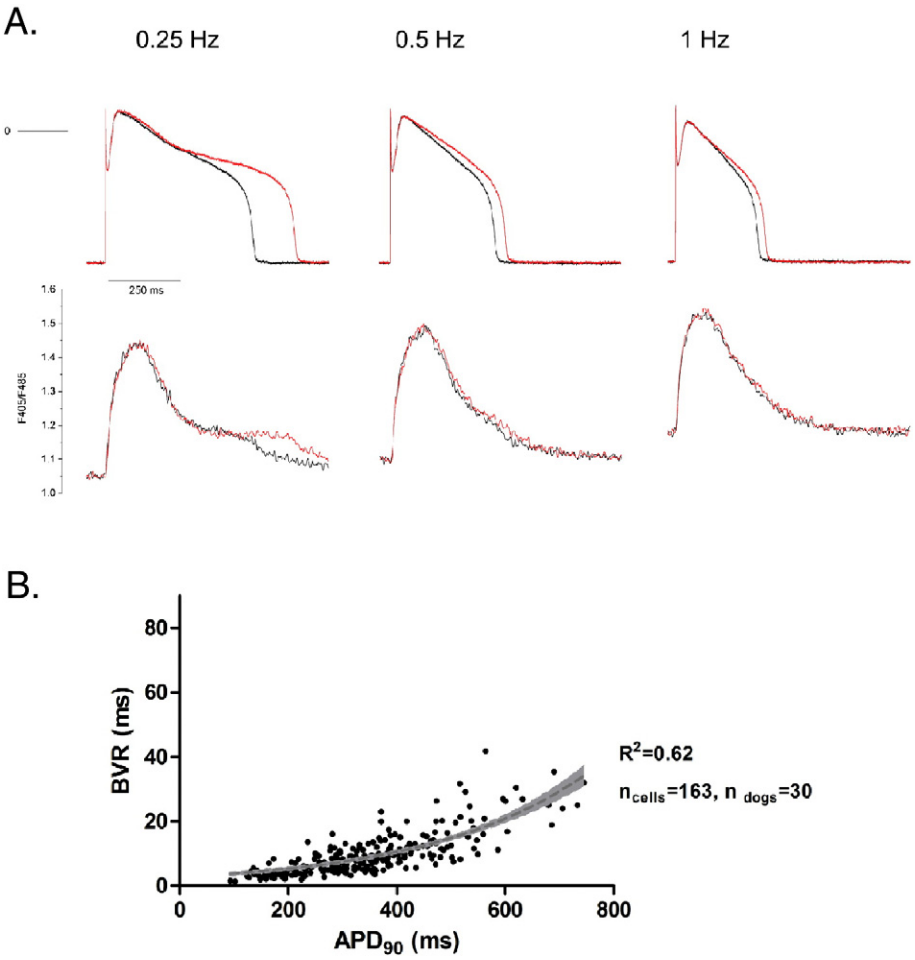


Fig. 1. Frequency dependence of BVR in CAVB myocytes. A. Representative examples of action potentials (AP) and Ca^{2+} transients recorded from the same LV CAVB myocyte during stimulation at 0.25, 0.5 and 1 Hz. Two consecutive APs and corresponding Ca^{2+} transients are shown for each frequency. B. BVR, quantified as short term variability, plotted as a function of APD90 at multiple pacing frequencies. Of note is the exponential relationship between APD90 and BVR. Shaded area indicates 95% confidence interval.

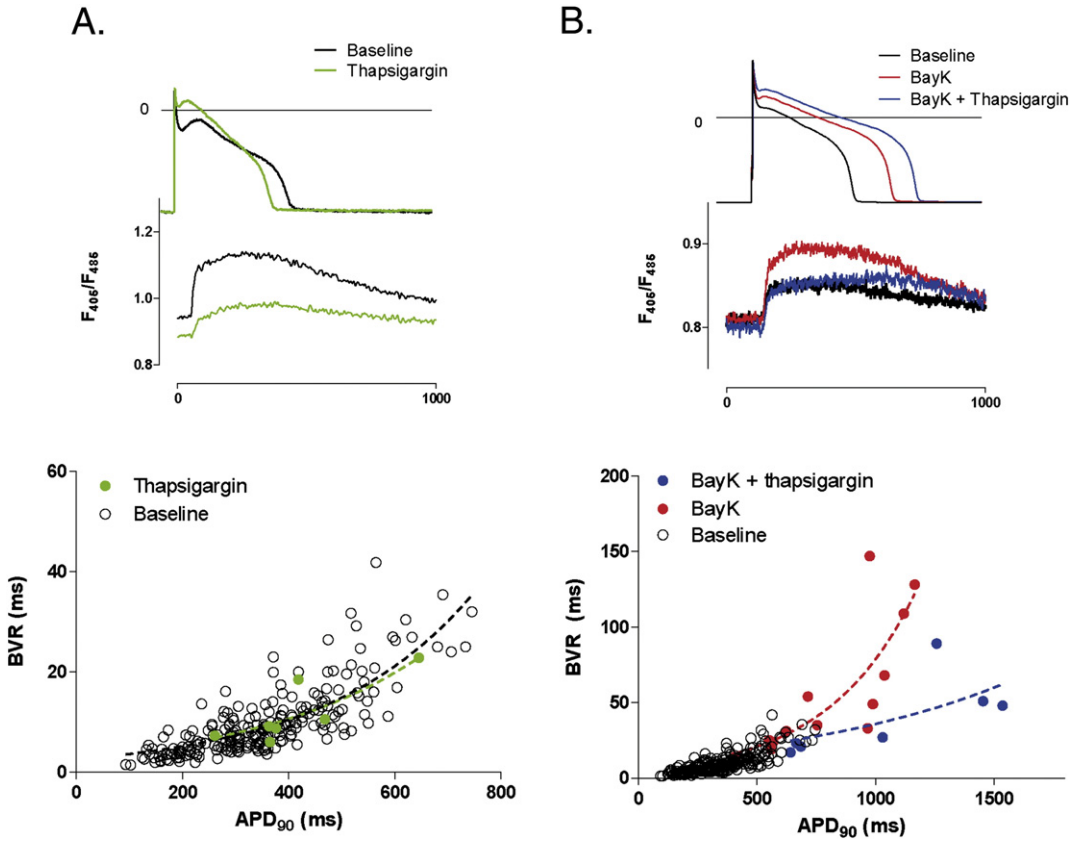


Fig. 2. Response of APD and BVR to suppression of Ca^{2+} release from the sarcoplasmic reticulum. A. Representative example of AP and Ca^{2+} transient recorded at 0.5 Hz under baseline conditions (black trace) and after thapsigargin (5 μM) perfusion (green trace). Grouped data are shown below with BVR as a function of APD90 (n = 7 cells for thapsigargin). B. Representative example showing prolongation of AP and increased Ca^{2+} transient recorded at 0.5 Hz after BayK8644 perfusion (red trace, compared to black trace at baseline). The subsequent effect of perfusion of thapsigargin in addition to BayK8644 is shown in blue. Grouped data are shown below with BVR as a function of APD90 (n = 14 cells for BayK8644 alone; n = 7 cells for BayK8644 + thapsigargin) are shown below, indicating that elimination of SR Ca^{2+} release, in the presence of an enhanced Ca^{2+} current can alter the APD/BVR relationship. Please note the differences in scale between the two graphs.

thapsigargin both global Ca^{2+} transient amplitude and APD were reduced. In this set of cells, pacing the myocytes at 0.5 Hz led to a reduction on average APD from 518 ± 48 ms to 414 ± 45 ms ($P < 0.05$; n = 7, N = 3), and BVR showed a similar reduction (from 21 ± 4.0 ms to 11.8 ± 2.4 ms, $P < 0.05$). Furthermore as shown in the bottom panel of Fig. 2A, the exponential relationship between APD and BVR was unchanged after thapsigargin treatment ($P = 0.25$).

To eliminate the effect of shortening the APD by thapsigargin we repeated these experiments in the presence of the LTCC agonist BayK8644 (1 μM). Perfusion of BayK8644 alone led to an increase in Ca^{2+} transient, APD, and BVR and the curve was steeper than under baseline conditions (Fig. 2B). On average, APD increased by 59 ± 10% (from 524 ± 37 ms to 834 ± 72 ms; $P < 0.05$, n = 14, N = 4) and BVR increased from 19.1 ± 1.7 ms to 56.2 ± 11.3 ms ($P < 0.05$). The addition of thapsigargin further prolonged APD (to 1039 ± 146 ms) whilst decreasing BVR (to 39.4 ± 9.7 ms). This intervention led to a significant shift in the exponential relationship between APD and BVR, meaning BVR was reduced for a given APD ($P < 0.001$; Fig. 2B).

To confirm our findings with BayK8644 and thapsigargin we carried out additional experiments with sustained caffeine applications (10 mM). At this concentration of caffeine, the SR will be initially depleted and thereafter will not be able to refill. While this is comparable to thapsigargin, the PDE inhibition by caffeine [29] raises cAMP and increases LTCC. In these experiments indeed APD was prolonged (on average by 52% (from 476 ± 21 ms to 743 ± 64 ms, n = 17). Meanwhile the APD/BVR relationship was significantly shifted to the right ($P < 0.001$), meaning that for a given APD, BVR was reduced when compared to baseline conditions (Fig. 3), which was qualitatively similar to our findings with BayK8644 and thapsigargin.

3.3. NCX inhibition reduces BVR via a reduction in APD in CAVB myocytes

As alterations in SR Ca^{2+} release drastically affect the APD/BVR relationship it would appear that a plateau current modulated by SR Ca^{2+} release, such as NCX or the LTCC, plays a major role in defining this relationship. Previous work has shown that NCX inhibition combined with LTCC inhibition is capable of attenuating dofetilide-induced increases in BVR in CAVB myocytes, however this was in the context of prolonged repolarization [24]. For these reasons we carried out further experiments to assess how NCX blockade, using SEA0400 (1 μM), would alter the APD/BVR relationship without the addition of I_{Kr} blockade. As shown in Fig. 4, inhibition of NCX, with concomitant LTCC blockade simultaneously reduces BVR and APD, however does not alter the relationship between these two entities ($P = 0.17$). APD was significantly reduced from 319 ± 16 ms to 264 ± 14 ms ($P < 0.05$), and BVR was also reduced from 10.0 ± 0.8 to 6.8 ± 0.5 ($P < 0.05$; n = 27, N = 8). SEA0400 perfusion also leads to an increase in the amplitude of the Ca^{2+} transient, as well as increasing diastolic Ca^{2+}. To investigate the relative contribution of NCX and LTCC in altering APD and BVR we utilized the fact that LTCC block by SEA-0400 is rapidly reversible on wash-out, whereas NCX block is not [30]. Interestingly when LTCC block was removed by washing out the compound in a subset of cells, APD and BVR returned to baseline levels (Supplemental Fig. 1),

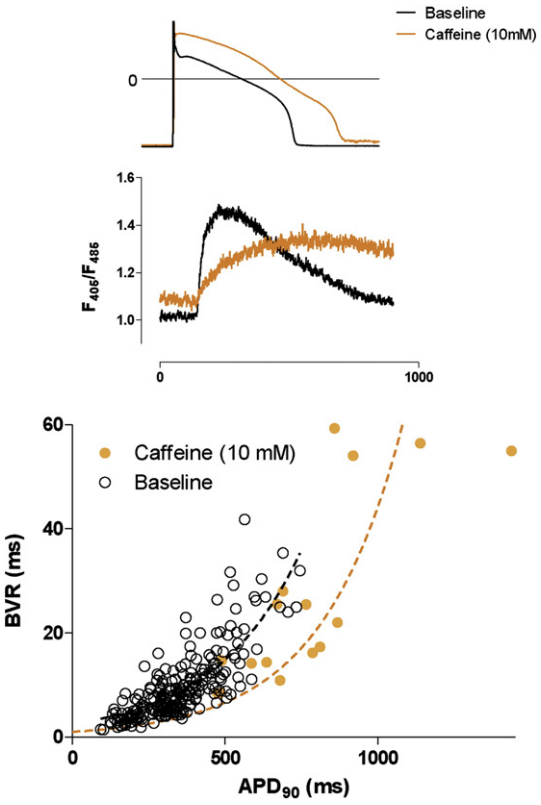


Fig. 3. Sustained caffeine application reduces BVR for a given APD. Representative example of AP and Ca^{2+} transient recorded at 0.5 Hz under baseline conditions (black trace) and with sustained caffeine (10 mM) perfusion (orange trace). Grouped data are shown below with BVR as a function of APD90 (n = 17 for caffeine).

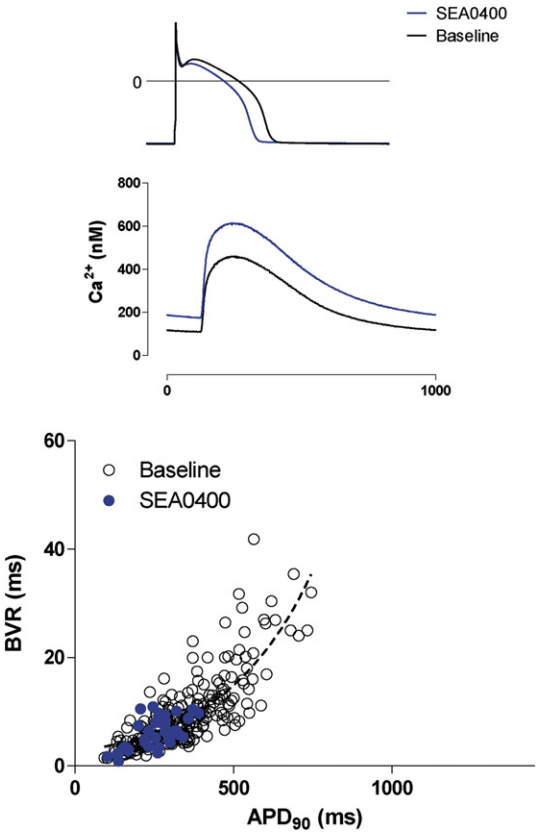


Fig. 4. NCX inhibition does not alter the APD/BVR relationship. Representative example of AP and Ca^{2+} transient recorded at 1 Hz under baseline conditions (black trace) and after SEA0400 (1 μM) perfusion (blue trace). Grouped data are shown below with BVR as a function of APD90 (n = 27 for SEA0400).

indicating that the decrease in these parameters seen with SEA0400 were LTCC-dependent.

3.4. Can variability of Ca^{2+} transients be induced with a steady state waveform?

We went on to investigate if variability in Ca^{2+} transients could be induced in voltage clamp experiments with a steady state waveform. As shown in Fig. 5 when a square voltage step is applied (of 1 s) to a CAVB myocyte, no variability in either the Ca^{2+} transient or the current that is provoked can be detected at this macroscopic level (right panel), indicating that differences that drive instability of the APD are small and not reflected in the global Ca^{2+} handling.

3.5. Local versus global Ca^{2+} control

Our experimental findings thus far indicated that Ca^{2+} release from the SR is able to modulate BVR, however no variability in the global Ca^{2+} transient at plateau phase could be detected in voltage clamp mode. For these reasons we went on to investigate if subsarcolemmal, as opposed to global, Ca^{2+} could be contributing to the exacerbated BVR in CAVB myocytes at longer APDs. As it is known that BAPTA has superior buffering capacities compared to EGTA in the subsarcolemmal space due to the fact that BAPTA is a faster Ca^{2+} chelator [31] we compared APDs and BVR after including either of these buffers in the internal pipette solution. As can be seen in Fig. 6 buffering Ca^{2+} with either agent caused a significant shift in the APD/BVR relationship ($P < 0.001$), however a significant difference is also observed between BAPTA (10 mM) and EGTA (10 mM), with BAPTA having the larger effect on the APD/BVR relationship when compared to EGTA ($P = 0.0038$). Hence for a given APD, BVR is lower after BAPTA, when compared to EGTA or baseline, indicating that subsarcolemmal Ca^{2+} plays a role in the exaggerated BVR seen at long APDs in CAVB.

4. Discussion

In the present study, we investigated the role that Ca^{2+}-dependent mechanisms play in the manifestation of BVR at the level of the single myocyte in a model of cardiac remodeling. The major findings of this study are: (i) After chronic AV block, BVR and APD are related in an exponential fashion, with a large increase in BVR at longer APDs; (ii) eliminating Ca^{2+} release from the SR shifts the APD/BVR relationship to the right, indicating that Ca^{2+}-release-dependent currents play a major role in the manifestation of BVR in this model; (iii) local dyadic Ca^{2+} concentrations contribute to a greater extent than global cytosolic Ca^{2+} concentrations in the control of BVR; and (iv) BVR is (window) LTCC dependent with subsarcolemmal Ca^{2+} as the dominant source. While (v) NCX inhibition with concomitant inhibition of I_{CaL} reduced both APD and BVR, this appears to be prominently driven by reduction of APD and LTCC current.

The present data extends earlier work [9] which demonstrated the role of altered Ca^{2+} handling on BVR under adrenergic stimulation in normal dog myocytes. Here we show that Ca^{2+} release during excitation-contraction coupling, as opposed to overload-induced diastolic release, has an effect on BVR in the absence of large-scale variability in the global Ca^{2+} transient. The present data support the notion that intricate changes in local Ca^{2+} can contribute to BVR in the setting of hypertrophy as in the CAVB model.

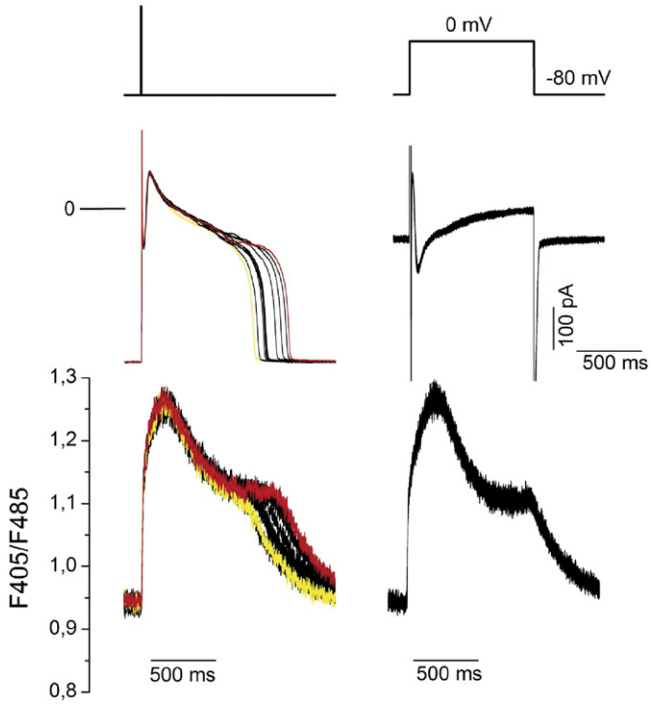


Fig. 5. Global Ca^{2+} variability is not seen when a fixed pulse is applied in voltage clamp mode. Representative example of AP and global Ca^{2+} transient recorded under current clamp conditions. Under these conditions variability at the level of the membrane current and the Ca^{2+} transient is observed. Red and yellow traces indicate longest and shortest APs and Ca^{2+} transients. If a square voltage pulse (−80 to 0 mV for 800 ms) is then applied despite the fact that the decline of the Ca^{2+} is delayed, variability is largely abolished.

4.1. APD and SR Ca^{2+} release contribute to BVR in CAVB myocytes

Previous work has proposed that BVR is a result of stochastic ion channel gating with I_{Kr} and I_{Na} playing a major role [10–12]. APD has been shown to be a major determinant of BVR and this also holds true in the present study in CAVB myocytes [6,12,32]. The theoretical APD/BVR relationship is exponential with large BVR at long APDs [13]. Although the pacing cycle length used in the majority of this study was slow (0.25 and 0.5 Hz), APDs observed were not exaggerated when compared to those seen in proarrhythmic situations, for example after IKr blockade [22]. Using slow pacing allowed for investigation of BVR during prolonged APDs without using pharmacological treatments.

The present findings indicate that SR Ca^{2+} release could be involved in the large BVR at long APD in the CAVB dog. Indeed, eliminating Ca^{2+} release and maintaining or increasing I_{CaL} using either sustained caffeine application or a combination of thapsigargin and BAYK8644 led to a decrease in BVR for a given APD. This was observed despite substantial global (slow) Ca^{2+} transient resulting from the enhanced Ca^{2+} influx.

However, variability in the peak of the Ca^{2+} transient was not evident in CAVB myocytes. Furthermore no variability in the global Ca^{2+} transient was observed when a fixed duration voltage step was applied. These data indicate that the variability in duration of the Ca^{2+} transient seen at the longest APDs is a result of the variability in the APD and its contributors, and not vice-versa. The influence of SR Ca^{2+} release on APD variability thus must result from small, presumably local, changes that are not detected in the global cytosolic Ca^{2+} signal.

This is further supported by the experiments where Ca^{2+} transients were suppressed. Buffering of Ca^{2+} using EGTA reduced BVR for a given APD whilst fast buffering with BAPTA had an even greater effect on the APD/BVR relationship. Our data is much in line with previous data showing that EGTA reduced baseline BVR in single guinea pig ventricular myocytes [6]. To our knowledge, however, we are the first to show that fast buffering has a greater influence on the APD/BVR relationship, further highlighting the importance of the local Ca^{2+} microdomain. The data are consistent with a recent study showing that BAPTA could alter BVR independently of APD [28]. Interestingly in the same study it was shown that increasing Ca^{2+} using a Ca^{2+} ionophore was able to increase BVR, again independently of the effect on APD [28]. Taken together these data demonstrate that BVR in CAVB occurs, at least in part, in response to membrane current variability, driven by local Ca^{2+} levels in the dyadic space.

4.2. Membrane currents regulated by dyadic cleft Ca^{2+} play a major role in determining BVR

A number of ion channels and exchanger proteins reside in the dyadic cleft and are under control of local Ca^{2+} concentration via a number of mechanisms. Alterations in activity of these channels, therefore, could be responsible for the Ca^{2+}-dependence of BVR.

One such possibility is I_{NCX}. Indeed previous work has shown that this current is increased in CAVB possibly due to an increase in intracellular Na^{+} [16]. The NCX inhibitor, SEA0400, has previously been shown to be able to reduce BVR in a number of experimental settings [7,24,32]. In the present study we have shown that SEA0400 does not alter the APD/BVR relationship when no other challenge on the repolarization reserve is present. Therefore the decrease in BVR seen with this compound cannot be separated from the APD reduction. The observation that on wash out of SEA0400, removing LTCC inhibition, APD and BVR returned to baseline levels, despite sustained NCX inhibition, further argues against a major role for NCX.

Recent data has also demonstrated that I_{NCX} inhibition with SEA0400 does not influence spatial heterogeneity in cytosolic Ca^{2+} decay [33]. Finally only a fraction of NCX appears to be tightly associated with the ryanodine receptors making it less likely that that this current would have major effects on BVR when local Ca^{2+} has an essential role [34]. In summary, although it is possible that I_{NCX} will contribute to some extent, by removal of Ca^{2+} from the dyadic space, the direct contribution of this current to BVR in CAVB appears to be small.

A second, and perhaps more likely candidate governing BVR is I_{CaL} and the I_{CaL} window current. This current arises within the window of overlap between the activation and inactivation of the channel and is dynamically modulated by Ca^{2+} in the dyadic space [17,35]. The current amplitude and the inactivation and recovery of LTCC during SR Ca^{2+} release, are larger in CAVB; this is a local process, unaffected by bulk cytosolic Ca^{2+} levels [17]. I_{CaL} window current is activated around the plateau voltages, where APD is most sensitive to fluctuations in duration and therefore will contribute to BVR [6]. Window I_{CaL} has also been implicated in the formation of early after depolarizations (EADs) [36]. Tanskanen et al. [45] carried out a modeling study elegantly illustrating that under β-adrenergic stimulation random fluctuations in the number of open LTCCs, particularly LTCCs in mode 2 gating, during the plateau phase of the AP can generate EADs. Theoretical analysis has further revealed that this current is required for ultralong APDs as well as being key to produce quasi-equilibrium states in the plateau voltage, promoting oscillatory behavior and EADs [37,38]. Whether BVR is a measure of the proportion of channels in mode 2 gating remains to be seen. Taking all the current data into consideration it is tempting to speculate that the modulation by SR Ca^{2+} release of window I_{CaL} may play a prominent role in the manifestation of BVR in CAVB.

In contrast to the present data, it was recently shown that when taking APD alterations into account, BAYK8644 leads to a reduction in BVR compared to baseline whilst inhibition of I_{CaL} with nisoldipine led to an APD independent increase in BVR [28]. This could be accounted for in a number of ways including incomplete LTCC block so window LTCC can still be activated or alterations in ion channel distribution and Ca^{2+} balance in CAVB. Additional experiments, such as investigating how BVR is altered by Ca^{2+} current inhibition when SR Ca^{2+} release is not present

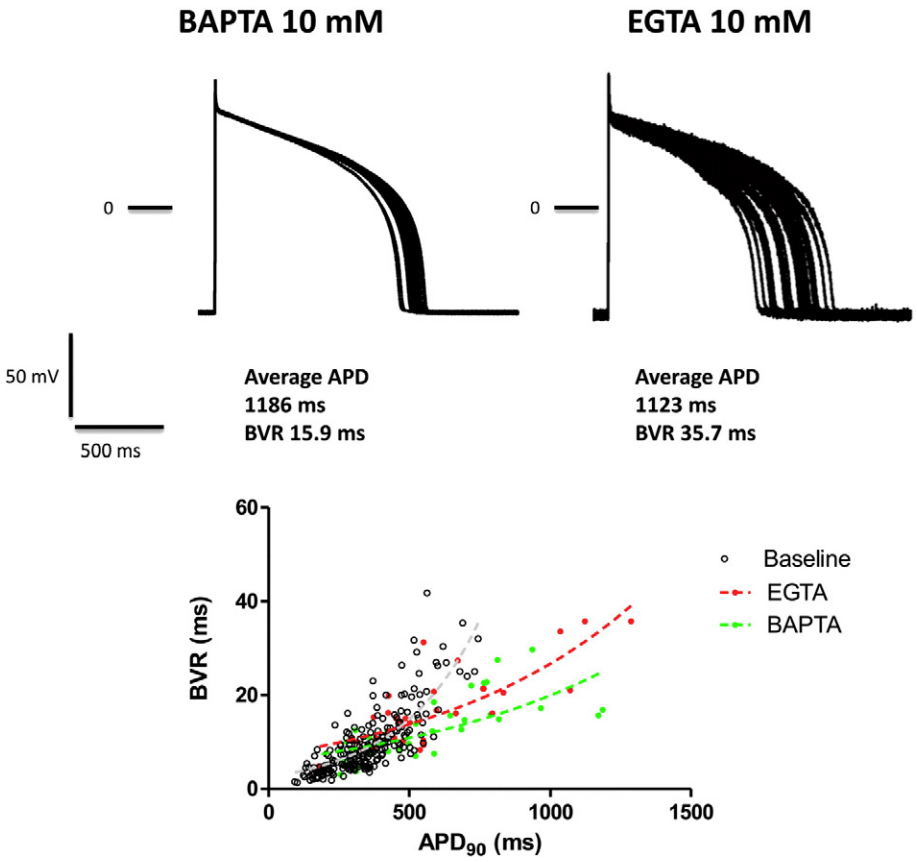


Fig. 6. Fast Ca^{2+} buffering reduces BVR for a given APD to a greater extent than cytosolic Ca^{2+} buffering. Representative examples showing 30 consecutive APs recorded either with BAPTA (10 mM) or EGTA (10 mM) in the internal pipette solution. Average APD and BVR values are indicated below for the specific cell. For equivalent APDs BVR is lower after BAPTA treatment when compared to EGTA. Grouped data are shown below with BVR as a function of APD90.

should be carried out to understand these apparent discrepancies however this is out of the scope of the present study.

4.3. Consequences for ventricular arrhythmogenesis?

BVR, at the level of the whole heart, is increased before the occurrence of arrhythmias in a number of animal models, as well as in certain patient populations, and although cellular BVR is unlikely to be the only determinant of BVR at the organ level it is thought to contribute [2,4,21]. The CAVB dog model was created to study repolarization dependent ventricular arrhythmias reproducibly. The model is characterized by 1) prolonged QT times with increased spatial and temporal dispersion, 2) increased stroke volume, and 3) biventricular hypertrophy. When comparing it to a clinical counterpart, the athlete's heart of endurance runners seems to the best fit. Interestingly recent work has shown that hearts of professional football players, where the rates of sudden cardiac death are 2–4 times more frequent than in age matched controls, also show an increased level of BVR [39]. The mechanism of the arrhythmias has further similarities with those occurring in the long QT syndrome and/or (in the transition) to heart failure. In the latter conditions, the arrhythmic parameter STV QT was clearly increased as has been shown to be the case in the CAVB dog model [40,41]. We have shown that alterations in SR Ca^{2+} release can modify BVR in single LV CAVB myocytes. Whether targeting this cellular phenomenon would result in reduced BVR and antiarrhythmic efficacy at the level of the whole organ remains to be seen. Nearly 20 years ago it was shown that blockade of Ca^{2+} release using ryanodine was able to reduce the occurrence of TdP in the CAVB model when the hearts were challenged with an I_{Kr} blocker together with abrupt changes in pacing frequency [42]. More recently it was also shown that either thapsigargin or ryanodine was able to suppress CAVB-induced EADs in a rabbit model of CAVB, although BVR was not recorded [43]. These agents all affect global Ca^{2+} release and therefore it would not be possible to use these as a therapeutic regimen, however perhaps more specific targeting of Ca^{2+} homeostasis would be an option. For example, a number of studies have explored the usefulness of CAMKII inhibition as an antiarrhythmic approach [44]. CaMKII-mediated LTCC phosphorylation has been shown to increase the likelihood of EADs [45], and previous work has shown that CAMKII inhibition can reduce BVR [7,25]. Additionally a recent study from our own group has shown that CAMKII can selectively modulate subpopulations of ryanodine receptors, located specifically in the dyadic cleft [46]. Whether the location specific control of Ca^{2+} release by CAMKII plays a role in BVR and arrhythmogenesis remains to be seen and the focus of ongoing work.

An additional question is how altering the I_{CaL} at one specific location on the membrane can influence the whole cell action potential. Previous work has shown that in healthy myocytes there are no differences in local APD magnitude and duration between the subsarcolemma and the T tubules [47]. More recent work from the same group showed that the electrical activity of a single T-tubule is also crucial in determining local Ca^{2+} release, and how this can be altered in diseased states due to the microarchitecture of the T-tubules [48]. Therefore one could assume that the alteration seen at one specific location would be conducted over the cell and alter the whole cell action potential. Further research at a higher electrical temporal and spatial resolution would be required to tease out the exact contributions.

Previous work from our own group has highlighted the fact that after chronic ischemia, T-tubules are lost, and Ca^{2+} heterogeneity is increased [49]. A recent study has also shown that BVR was increased in a model of premature ventricular contraction (PVC) induced cardiomyopathy [50]. Together with the increases in BVR observed in this study, structural integrity of the T-tubules and the dyad was also altered

and Cav1.2 protein was relocated away from the T-tubules in myocytes in this model. These data indicate that there may be a link between structural integrity, local Ca^{2+}, LTCC activation and BVR in other pathophysiological remodeling Future research should therefore concentrate on associations between structure and function with regard to enhanced BVR in such models.

4.4. Limitations

A potential limitation of the present study is that the majority of the work carried out has utilized pharmacological agents that may have nonspecific effects on membrane conductance and ultimately BVR. To minimize the risk of this we chose specific concentrations of the compounds, and we repeated experiments using different agents converging on the same Ca^{2+} pathways. The fact that agents that do converge on the same pathways give qualitatively similar data with regard to their APD/BVR relationships supports our hypotheses.

A second limitation is the resolution of the Ca^{2+} transient recordings. Using the techniques employed in this study it was not possible to pick up any spatial heterogeneity in Ca^{2+} release (or reuptake), which could possibly have provided additional information regarding the origin of BVR seen in CAVB. Preliminary data using confocal Ca^{2+} imaging in CAVB myocytes (Supplemental data) indicate that there is substantial variability in the local Ca^{2+} transient at sites where Ca^{2+} release is coupled to the sarcolemmal membrane at the early stage of the AP. The point at which AP divergence is initiated also occurs early. Taken together these data further strengthen our conclusions regarding local Ca^{2+} influencing BVR, whilst also indicating that the variability in local Ca^{2+} has a spatial aspect which coincides with the location of Ca^{2+} entry, possible through the LTCC. Additional work will concentrate on this aspect and how alterations in this parameter may drive BVR.

4.5. Conclusion

We have shown that there is an exponential relationship between APD and BVR in hypertrophied myocytes, and that this relationship is strongly dependent on SR Ca^{2+} release, modulating the (window) L-type Ca^{2+} currents in the subsarcolemmal space. Specifically controlling subsarcolemmal Ca^{2+} could therefore be an interesting target for reducing BVR and ultimately arrhythmia occurrence. Further research will concentrate on isolating the currents involved and investigate subsarcolemmal Ca^{2+} levels to directly assess the contribution to elevated BVR levels seen in cardiac remodeling.

Sources of funding

The work was supported by European Union grant Health-F2-2009-241526 EUTrigTreat (to KRS and MAV), the Interuniversity Attraction Poles (IAP P7/10) Program, Belgium (to GA, KRS and MAV), and the Research Foundation Flanders (FWO-Vlaanderen, postdoctoral Fellowship, to DMJ and to IL; PhD fellowship to ED).

Disclosures

None.

Acknowledgments

The authors wish to thank Dr. Lars Kattner and Dr. Eric Rauch, Endotherm GmbH for synthesizing and supplying SEA0400, and Prof. Piet Claus for advice on statistics.

Appendix A. Supplementary data

Supplementary data to this article can be found online at http://dx.doi.org/10.1016/j.yjmcc.2015.10.008.

References

[1] M.B. Thomsen, S.C. Verduyn, M. Stengl, J.D.M. Beekman, G. de Pater, J. van Opstal, et al., Increased short-term variability of repolarization predicts d-sotalol-induced torsades de pointes in dogs, Circulation 110 (16) (2004 Oct 19) 2453–2459.
[2] M. Hinterseer, M.B. Thomsen, B.-M. Beckmann, A. Pfeufer, R. Schimpf, H.-E. Wichmann, et al., Beat-to-beat variability of QT intervals is increased in patients with drug-induced long-QT syndrome: a case control pilot study, Eur. Heart J. 29 (2) (2008 Jan) 185–190.
[3] V. Floré, P. Claus, G. Antoons, P. Oosterhoff, P. Holemans, M.A. Vos, et al., Microvolt T-wave alternans and beat-to-beat variability of repolarization during early postischemic remodeling in a pig heart, Heart Rhythm. 8 (7) (2011 Jul) 1050–1057.
[4] D.J. Gallacher, A. Van de Water, H. van der Linde, A.N. Hermans, H.R. Lu, R. Towart, et al., In vivo mechanisms precipitating torsades de pointes in a canine model of drug-induced long-QT1 syndrome, Cardiovasc. Res. 76 (2) (2007 Nov 1) 247–256.
[5] L. Carlsson, B. Andersson, G. Linhardt, L. Löfberg, Assessment of the ion channel-blocking profile of the novel combined ion channel blocker AZD1305 and its proarrhythmic potential versus dofetilide in the methoxamine-sensitized rabbit in vivo, J. Cardiovasc. Pharmacol. 54 (1) (2009 Jul) 82–89.
[6] M. Zaniboni, A.E. Pollard, L. Yang, K.W. Spitzer, Beat-to-beat repolarization variability in ventricular myocytes and its suppression by electrical coupling, Am. J. Physiol.-Heart Circ. Physiol. 278 (3) (2000) H677–H687.
[7] D.M. Johnson, J. Heijman, C.E. Pollard, J.-P. Valentin, H.J.G.M. Crijns, N. Abi-Gerges, et al., IKs restricts excessive beat-to-beat variability of repolarization during beta-adrenergic receptor stimulation, J. Mol. Cell. Cardiol. 48 (1) (2010 Jan) 122–130.
[8] P.G.A. Volders, M. Stengl, J.M. van Opstal, U. Gerlach, R.L.H.M.G. Spätjens, J.D.M. Beekman, et al., Probing the contribution of IKs to canine ventricular repolarization: key role for beta-adrenergic receptor stimulation, Circulation 107 (21) (2003 Jun 3) 2753–2760.
[9] D.M. Johnson, J. Heijman, E.F. Bode, D.J. Greensmith, H. van der Linde, N. Abi-Gerges, et al., Diastolic spontaneous calcium release from the sarcoplasmic reticulum increases beat-to-beat variability of repolarization in canine ventricular myocytes after adrenergic stimulation, Circ. Res. 112 (2) (2012 Nov 13) 246–256.
[10] L. Wu, J. Ma, H. Li, C. Wang, E. Grandi, P. Zhang, et al., Late sodium current contributes to the reverse rate-dependent effect of IKr inhibition on ventricular repolarization, Circulation 123 (16) (2011 Apr 11) 1713–1720.
[11] E. Pueyo, A. Corrias, L. Virág, N. Jost, T. Szél, A. Varró, et al., A multiscale investigation of repolarization variability and its role in cardiac arrhythmogenesis, Biophys. J. 101 (12) (2011 Dec 21) 2892–2902.
[12] M. Lemay, E. de Lange, J.P. Kucera, Effects of stochastic channel gating and distribution on the cardiac action potential, J. Theor. Biol. 281 (1) (2011 Jul 21) 84–96.
[13] J. Heijman, A. Zaza, D.M. Johnson, Y. Rudy, R.L.M. Peeters, P.G.A. Volders, et al., Determinants of beat-to-beat variability of repolarization duration in the canine ventricular myocyte: a computational analysis, PLoS Comput. Biol. 9 (8) (2013 Aug 22), e1003202 (McCulloch AD, editor).
[14] A. Oros, J.D.M. Beekman, M.A. Vos, The canine model with chronic, complete atrioventricular block, Pharmacol. Ther. 119 (2) (2008 Aug) 168–178.
[15] P.G. Volders, K.R. Sipido, M.A. Vos, R.L. Spätjens, J.D. Leunissen, E. Carmeliet, et al., Downregulation of delayed rectifier K(+) currents in dogs with chronic complete atrioventricular block and acquired torsades de pointes, Circulation 100 (24) (1999 Dec 14) 2455–2461.
[16] Sipido KR, Volders PGA, Groot SHM de, Verdonck F, Werf FV de, Wellens HJJ, et al. Enhanced Ca2+ release and Na/Ca exchange activity in hypertrophied canine ventricular myocytes potential link between contractile adaptation and arrhythmogenesis. Circulation. 2000 Oct 24;102(17):2137–44.
[17] G. Antoons, P.G.A. Volders, T. Stankovicova, V. Bito, M. Stengl, M.A. Vos, et al., Window Ca2+ current and its modulation by Ca2+ release in hypertrophied cardiac myocytes from dogs with chronic atrioventricular block, J. Physiol. 579 (1) (2007 Feb 15) 147–160.
[18] S.H.M. De Groot, M. Schoenmakers, M.M.C. Molenschot, J.D.M. Leunissen, H.J.J. Wellens, M.A. Vos, Contractile adaptations preserving cardiac output predispose the hypertrophied canine heart to delayed afterdepolarization-dependent ventricular arrhythmias, Circulation 102 (17) (2000 Oct 24) 2145–2151.
[19] E. Detre, M.B. Thomsen, J.D. Beekman, K.-U. Petersen, M.A. Vos, Decreasing the infusion rate reduces the proarrhythmic risk of NS-7: confirming the relevance of short-term variability of repolarisation in predicting drug-induced torsades de pointes, Br. J. Pharmacol. 145 (3) (2005 Jun) 397–404.
[20] Johnson DM, de Jong MMJ, Crijns HJGM, Carlsson LG, Volders PGA. Reduced ventricular proarrhythmic potential of the novel combined ion-channel blocker AZD1305 versus dofetilide in dogs with remodeled hearts. Circ Arrhythm Electrophysiol. 2011 Nov 11;5(1):201–9.
[21] M.B. Thomsen, P.G.A. Volders, J.D.M. Beekman, J. Matz, M.A. Vos, Beat-to-beat variability of repolarization determines proarrhythmic outcome in dogs susceptible to drug-induced torsades de pointes, J. Am. Coll. Cardiol. 48 (6) (2006 Sep 19) 1268–1276.
[22] G. Antoons, A. Oros, J.D.M. Beekman, M.A. Engelen, M.J.C. Houtman, L. Belardinelli, et al., Late Na+ current inhibition by ranolazine reduces torsades de pointes in the chronic atrioventricular block dog model, J. Am. Coll. Cardiol. 55 (8) (2010 Feb 23) 801–809.
[23] A. Oros, M.J. Houtman, P. Neco, A.M. Gomez, S. Rajamani, P. Oosterhoff, et al., Robust anti-arrhythmic efficacy of verapamil and flunarizine against dofetilide-induced TdP arrhythmias is based upon a shared and a different mode of action, Br. J. Pharmacol. 161 (1) (2010 Sep) 162–175.
[24] V.J.A. Bourgonje, M.A. Vos, S. Ozdemir, N. Doisne, K. Acsai, A. Varro, et al., Combined Na+/Ca2+ exchanger and L-type calcium channel block as a potential strategy to

suppress arrhythmias and maintain ventricular function, Circ. Arrhythm. Electrophysiol. 6 (2) (2013 Mar 20) 371–379.
[25] V.J.A. Bourgonje, M. Schoenmakers, J.D.M. Beekman, R. van der Nagel, M.J.C. Houtman, L.F. Miedema, et al., Relevance of calmodulin/CaMKII activation for arrhythmogenesis in the AV block dog, Heart Rhythm. 9 (11) (2012 Nov) 1875–1883 (e2).
[26] M. Stengl, C. Ramakers, D.W. Donker, A. Nabar, A.V. Rybin, R.L.H.M.G. Spätjens, et al., Temporal patterns of electrical remodeling in canine ventricular hypertrophy: focus on IKs downregulation and blunted β-adrenergic activation, Cardiovasc. Res. 72 (1) (2006 Oct 1) 90–100.
[27] M. Schoenmakers, C. Ramakers, J.M. van Opstal, J.D.M. Leunissen, C. Londoño, M.A. Vos, Asynchronous development of electrical remodeling and cardiac hypertrophy in the complete AV block dog, Cardiovasc. Res. 59 (2) (2003 Aug 1) 351–359.
[28] N. Szentandrássy, K. Kistamás, B. Hegyi, B. Horváth, F. Ruzsnavszky, K. Váczi, et al., Contribution of ion currents to beat-to-beat variability of action potential duration in canine ventricular myocytes, Pflugers Arch. - Eur. J. Physiol. 2 (2014 Aug) 1–13.
[29] R.W. Butcher, E.W. Sutherland, Adenosine 3′,5′-phosphate in biological materials. I. Purification and properties of cyclic 3′,5′-nucleotide phosphodiesterase and use of this enzyme to characterize adenosine 3′,5′-phosphate in human urine, J. Biol. Chem. 237 (1962 Apr) 1244–1250.
[30] S. Ozdemir, V. Bito, P. Holemans, L. Vinet, J.-J. Mercadier, A. Varro, et al., Pharmacological inhibition of Na/Ca exchange results in increased cellular Ca2+ load attributable to the predominance of forward mode block, Circ. Res. 102 (11) (2008 May 8) 1398–1405.
[31] Y. You, D.J. Pelzer, S. Pelzer, Modulation of L-type Ca2+ current by fast and slow Ca2+ buffering in guinea pig ventricular cardiomyocytes, Biophys. J. 72 (1) (1997 Jan) 175–187.
[32] P. Milberg, C. Pott, M. Fink, G. Frommeyer, T. Matsuda, A. Baba, et al., Inhibition of the Na+/Ca2+ exchanger suppresses torsades de pointes in an intact heart model of long QT syndrome-2 and long QT syndrome-3, Heart Rhythm Off. J. Heart Rhythm Soc. 5 (10) (2008 Oct) 1444–1452.
[33] F. Hohendanner, S. Ljubojevic, N. MacQuaide, M. Sacherer, S. Sedej, L. Biesmans, et al., Intracellular dyssynchrony of diastolic cytosolic [Ca2+] decay in ventricular cardiomyocytes in cardiac remodeling and human heart failure, Circ. Res. 113 (5) (2013 Jul 3) 527–538.
[34] K.R. Sipido, H. Cheng, T-tubules and ryanodine receptor microdomains: on the road to translation, Cardiovasc. Res. 98 (2) (2013 May 1) 159–161.
[35] Y. Hirano, A. Moscucci, C.T. January, Direct measurement of L-type Ca2+ window current in heart cells, Circ. Res. 70 (3) (1992 Mar) 445–455.
[36] P.G. Volders, M.A. Vos, B. Szabo, K.R. Sipido, S.H. de Groot, A.P. Gorgels, et al., Progress in the understanding of cardiac early afterdepolarizations and torsades de pointes: time to revise current concepts, Cardiovasc. Res. 46 (3) (2000 Jun) 376–392.
[37] Z. Qu, D. Chung, Mechanisms and determinants of ultralong action potential duration and slow rate-dependence in cardiac myocytes, PLoS One 7 (8) (2012), e43587.
[38] Qu Z, Xie L-H, Olcese R, Karagueuzian HS, Chen P-S, Garfinkel A, et al. Early afterdepolarizations in cardiac myocytes: beyond reduced repolarization reserve. Cardiovasc. Res. 2013 Jul 1;99(1):6–15.
[39] C. Lengyel, A. Orosz, P. Hegyi, Z. Komka, A. Udvardy, E. Bosnyák, et al., Increased short-term variability of the QT interval in professional soccer players: possible implications for arrhythmia prediction, PLoS One 6 (4) (2011 Apr 15), e18751.
[40] M. Hinterseer, B.-M. Beckmann, M.B. Thomsen, A. Pfeufer, M. Ulbrich, M.F. Sinner, et al., Usefulness of short-term variability of QT intervals as a predictor for electrical remodeling and proarrhythmia in patients with nonischemic heart failure, Am. J. Cardiol. 106 (2) (2010 Jul 15) 216–220.
[41] M. Hinterseer, B.-M. Beckmann, M.B. Thomsen, A. Pfeufer, R. Dalla Pozza, M. Loeff, et al., Relation of increased short-term variability of QT interval to congenital long-QT syndrome, Am. J. Cardiol. 103 (9) (2009 May 1) 1244–1248.
[42] S.C. Verduyn, M.A. Vos, A.P. Gorgels, J. van der Zande, J.D. Leunissen, H.J. Wellens, The effect of flunarizine and ryanodine on acquired torsades de pointes arrhythmias in the intact canine heart, J. Cardiovasc. Electrophysiol. 6 (3) (1995) 189–200.
[43] X. Qi, Y.-H. Yeh, D. Chartier, L. Xiao, Y. Tsuji, B.J.J.M. Brundel, et al., The calcium/calmodulin/kinase system and arrhythmogenic afterdepolarizations in bradycardia-related acquired long-QT syndrome, Circ. Arrhythm. Electrophysiol. 2 (3) (2009 Jun) 295–304.
[44] L.S. Maier, Experimental antiarrhythmic targets: CaMKII inhibition — ready for clinical evaluation? Curr. Med. Chem. 21 (11) (2014) 1299–1307.
[45] A.J. Tanskanen, J.L. Greenstein, B. O'Rourke, R.L. Winslow, The role of stochastic and modal gating of cardiac L-type Ca2+ channels on early after-depolarizations, Biophys. J. 88 (1) (2005 Jan) 85–95.
[46] E. Dries, V. Bito, I. Lenaerts, G. Antoons, K.R. Sipido, N. Macquaide, Selective modulation of coupled ryanodine receptors during microdomain activation of calcium/calmodulin-dependent kinase II in the dyadic cleft, Circ. Res. 113 (11) (2013 Sep 30) 1242–1252.
[47] L. Sacconi, C. Ferrantini, J. Lotti, R. Coppini, P. Yan, L.M. Loew, et al., Action potential propagation in transverse-axial tubular system is impaired in heart failure, Proc. Natl. Acad. Sci. U. S. A. 109 (15) (2012 Apr 10) 5815–5819.
[48] C. Crocini, R. Coppini, C. Ferrantini, P. Yan, L.M. Loew, C. Tesi, et al., Defects in T-tubular electrical activity underlie local alterations of calcium release in heart failure, Proc. Natl. Acad. Sci. 111 (42) (2014 Oct 21) 15196–15201.
[49] F.R. Heinzel, V. Bito, L. Biesmans, M. Wu, E. Detre, F. von Wegner, et al., Remodeling of T-tubules and reduced synchrony of Ca2+ release in myocytes from chronically ischemic myocardium, Circ. Res. 102 (3) (2008 Feb 15) 338–346.
[50] Y. Wang, J.M. Eltit, K. Kaszala, A. Tan, M. Jiang, M. Zhang, et al., Cellular mechanism of premature ventricular contraction-induced cardiomyopathy, Heart Rhythm. 11 (11) (2014 Nov) 2064–2072.